



Sodium Alginate Substrate Coated with PVA/Nanosilver Composite Nanofibers for Skin Tissue Engineering

Ishraq Abd Ulrazzaq Kadhim¹, Alaa Sabeh Taeh², Mayyadah S. Abed^{1*}

¹ Department of Materials of Engineering, University of Technology-Iraq, Baghdad 10066, Iraq

² Department of Architectural Engineering, University of Wasit, Wasit 5200, Iraq

Corresponding Author Email: Mayyadah.S.Abed@uotechnology.edu.iq

Copyright: ©2024 The authors. This article is published by IIETA and is licensed under the CC BY 4.0 license (<http://creativecommons.org/licenses/by/4.0/>).

<https://doi.org/10.18280/rcma.340305>

ABSTRACT

Received: 25 December 2023

Revised: 28 April 2024

Accepted: 12 May 2024

Available online: 22 June 2024

Keywords:

nanofibers, sodium alginate, silver nanoparticles, electrospinning, skin tissue engineering

The established potential of sodium alginate (SA) in tissue engineering and regenerative medicine underscores its significance. This study involved coating a sodium alginate substrate (SA) with nanofibers through the electrospinning of a polyvinyl alcohol (PVA) solution loaded with various antimicrobial agents, specifically silver nanoparticles (AgNPs). The coated nanofibers underwent comprehensive physicochemical, biological, and morphological characterization. The analysis of the coated nanofibers included techniques such as Field Emission Scanning Electron Microscopy (FESEM) and Fourier Transform Infrared Spectroscopy (FTIR). The contact angle was measured using the sessile drop method. Microbiological assays were conducted to evaluate the effectiveness against *Staphylococcus aureus* (*S. aureus*). Additionally, cell viability was assessed using MTT assays on the AD-MSC cell line. In vitro assays demonstrated the excellent biocompatibility of the coated nanofibers in cell culture. The SA/PVA/AgNPs-coated nanofibers exhibited inhibitory effects on the growth and proliferation of *Staphylococcus aureus* bacteria. The findings suggest that these novel coated nanofibers hold promise for the development of sustainable biomaterials for skin tissue engineering.

1. INTRODUCTION

As emerging biomedical disciplines, tissue engineering and regenerative medicine offer innovative methods for the regeneration and healing of damaged tissue [1, 2]. Over the past several decades, tissue engineering research has increased significantly. Its achievements have encompassed a wide range of investigations, such as surface inspection, biomaterial development and processing, and the functionalization for improved imaging and cell-material interactions [3, 4]. Tissue engineering, a key component of regenerative medicine, uses the principles of cell transplantation, engineering, and material science to repair, regenerate, or restore the functionality of injured or destroyed tissues. In order to achieve this, either alone or in combination, cells, biomaterials, and biochemical components are utilized [5, 6]. It employs basic chemistry to regulate the fate of cells inside a scaffold, a supportive matrix that, by mechanical and biological means, promotes cell adhesion, migration, proliferation, and attachment into tissues [7, 8].

Due to its exceptional biocompatibility, sodium alginate stands out as one of the frequently employed natural biopolymers in tissue engineering. Alginates, derived from the alginic acid present in the brown cell walls of seaweed, are polysaccharides with diverse ratios of -D-manuronic acid (M) and -L-guluronic acid (G) sequences, as well as varying molecular weights. Notably, sodium alginate is water-soluble,

possesses hemostatic properties, and can effectively absorb body fluids [9-12].

In the biomedical domain, polyvinyl alcohol (PVA) finds extensive use owing to its biocompatibility and non-toxic nature. It proves to be a valuable choice for crafting synthetic cartilage due to its suitable moisture content and controllable mechanical characteristics [13]. Notably, natural materials like hyaluronic acid, chitosan, and cartilage acellular matrix exhibit a heightened inclination for cell-to-tissue and cell-to-cell interactions. This unique feature enables biomaterials to closely emulate in vivo functions and tissue architecture [14, 15].

The electrospinning process enables the production of metal nanoparticle-based coated nanomaterials, composites, and inorganic agents for wound treatment. Nanofibers, formed through this process, exhibit distinctive characteristics owing to their unique surface-area-to-volume ratio and the ability to generate porous and interconnected structures. Additionally, these nanofibers are composed of natural biopolymers, mirroring the structure of the extracellular matrix (ECM) [16, 17].

The large specific surface area and high interconnectivity of electrospun nanofiber scaffolds can help promote the extracellular matrix (ECM)-cell contact at the site of damage. They also have various cell binding sites and good mechanical strength due to their porous three-dimensional structure [18]. Nowadays, a growing amount of research is being done on the

fabrication of composite scaffolds for the treatment of drug-resistant bacteria and wounds that are difficult to cure utilizing metal-based nanoparticles and electrospinning technologies. Metal-based nanoparticles' innate biological capabilities can give scaffolds special material and biological characteristics. In the future, this kind of bionanomaterial is anticipated to play a significant role in the biomedical area as a therapeutic approach and material selection, offering novel and distinctive solutions for treating wounds that are difficult to heal and preventing bacterial infections [19].

However, because metal nanoparticles have unique biological effects and physicochemical properties, regulatory agencies need to evaluate their efficacy and safety as functional components of medicinal products [20].

Silver nanoparticles, due to their excellent antibacterial activity, have garnered significant attention for use in antibacterial applications. Notably, silver ions (Ag^+) are considered crucial to the antibacterial response, with some researchers asserting that Ag^+ exhibits the strongest antibacterial activity among all metal ions. Silver nanoparticles can help control damage to bacterial cellular components by reactive oxygen species (ROS) [17, 21].

The antibacterial mechanism of silver nanoparticles as of right now is summarized as follows: AgNPs cause bacterial intracellular structures to collapse, releasing Ag^+ into the cytoplasm where it binds to proteins in a specific way to inactivate enzymes. AgNPs also cause permeability and structural alterations in bacteria, which deplete proton power and damage cell membranes. AgNPs rip apart and permeate bacterial cell walls and membranes to demolish their structure [22, 23].

Despite the limited information regarding their toxicity and in vivo biological activity, silver nanoparticles (AgNPs) have been employed extensively as antimicrobial agents in healthcare, skincare products, food storage, fabric coatings, and various environmental applications for a considerable duration. Characterized by sizes ranging from 1 nm to 100 nm, AgNPs belong to the class of zero-dimensional materials and exhibit distinct morphologies [24, 25].

The objective of this study was to develop sustainable coated nanofibers incorporating silver antimicrobial agents (AgNPs) by blending them with polyvinyl alcohol (PVA) and depositing the mixture as electrospun coated nanofibers on sodium alginate film substrates. To assess the potential use of

these coated nanostructures as viable biomaterials for skin regeneration, the research involved an investigation into the morphological aspects (scanning electron microscopy SEM), structural characteristics (Fourier Transform Infrared spectroscopy FTIR), and biological features of the coated nanostructures.

2. EXPERIMENTAL WORK

2.1 Materials used

Sodium alginate, a natural biopolymer with medium molecular weight, was sourced from Xian in Shaanxi, China. The biopolymer polyvinyl alcohol, also of medium molecular weight, was synthesized using materials from CDH in India. Silver nanoparticles (AgNPs) with particle sizes of 20 nm were obtained from Hongwn International Group in China. Distilled water was used in the synthesis process.

2.2 Preparing substrate for nanofibers coating

Sodium alginate (SA) films measuring $8 \times 8 \text{ cm}^2$ were produced using the solvent casting technique. In this method, sodium alginate (4gm) was dissolved in distilled water (100 ml) at a concentration of 4% w/v. The dissolution process occurred under a magnetic stirrer operating at 1200 rpm and at a temperature of 60°C for 1 hour. Following the removal of bubbles, the solution was cast into a Petri dish and then dried for 3 hours at 50°C . This drying process aimed to create uniform sodium alginate films suitable for the precipitation of coating nanostructures. The resulting films were designated as FA, denoting their sodium alginate content of 4%.

2.3 Preparing of nanofibers coating

Figure 1 illustrates the process for preparing a nanostructure coating on a sodium alginate (SA) substrate. Figure 2 showed the samples that prepared. The procedure involved the creation of an electrospinning solution using the biopolymer polyvinyl alcohol (PVA). The PVA (7gm) was dissolved in distilled water (100 ml) at a concentration of 7% w/v. This solution was stirred with a magnetic stirrer at 1200 rpm and 100°C for one hour to achieve a homogeneous mixture.

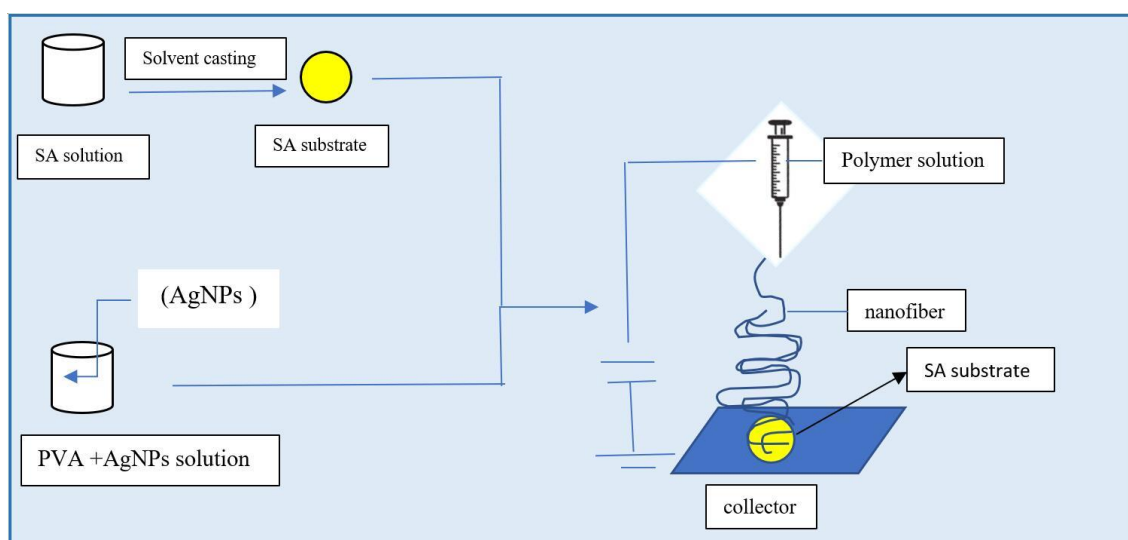


Figure 1. Schematic for preparation of nanofibers coating on substrate (SA)



Figure 2. Image of scaffolds

Note: (1) FA (4%Alg); (2) FA1 (4%Alg+7%PVA); (3) FA2 (4%Alg+7%PVA+0.1%wt AgNPS); (4) FA3 (4%Alg+7%PVA+0.2%wt AgNPS); (5) FA4 (4%Alg+7%PVA+0.3%wt AgNPS)

To incorporate silver nanoparticles (AgNPs), incremental amounts (0.1, 0.2, 0.3 g) were added to the polyvinyl alcohol solution. A coating solution (30 ml) for electrospinning was then prepared using an ultrasonic stirrer, agitating at 1400 rpm for 1 hour at room temperature until the desired viscosity was attained.

The resulting electrospinning solution (5 ml), devoid of bubbles, was loaded into a syringe and electrospun onto sodium alginate films. The electrospinning process took place at a distance of 15 cm between the needle and the collector, with a supply voltage of 25 V and a flow rate of 1 ml/h. The coated nanostructure on the sodium alginate substrate was left to dry completely at room temperature. Table 1 provides detailed parameters for the nanofiber coating on sodium alginate films.

Table 1. Parameter of nanofibers coating on substrate (SA)

No.	Alginate %	PVA %	AgNPs (g)
FA	4%	-	-
FA1	4%	7%	-
FA2	4%	7%	0.1
FA3	4%	7%	0.2
FA4	4%	7%	0.3

2.4 Characterizations and inspection assay

2.4.1 Field Emission Scanning Electron Microscopy (SEM)

Field Emission Scanning Electron Microscopy (FESEM) was employed for the observation of fiber and diameter sizes of the coated nanostructures, utilizing the MIRAI model from Tescan in the Czech Republic. Prior to testing, the samples underwent an automated coating process with conductive layers of gold. This coating was achieved using a Q 150R ES sputter coater from Quorum in East Sussex, UK. The sample surface was coated with conductive layer using magnetron-generated argon plasma to improve the samples' conductivity and guaranteeing precise imaging throughout the FESEM examination.

2.4.2 Fourier transform infrared analysis

The mid-infrared spectra of electrospun nanostructures were gained using German-based Bruker Optics Corporation equipment. The used resolution was 4 cm^{-1} within frequency range of 4000 to 700 cm^{-1} . The experimental process was carried out three times to enhance the accuracy and

consistency of the spectral data. The objective of this analytical method was to offer comprehensive understandings of the molecular makeup and structural properties of the electrospun nanostructures containing antimicrobial chemicals on the AS layer.

2.4.3 In vitro evaluation of biocompatibility

Briefly, AD-MSC cells were seeded into a 96-well tissue culture plate and cultivated for 24 hours in 100 μl of DMEM/F12 supplemented with 10% heat-inactivated fetal bovine serum (FBS). Afterward, the culture medium was ten replaced with a new fresh, serum-free solution containing increasing higher dilutions of the sample, and the cells were incubated for four hours.

The media were then switched to 100 μl of complete media and left for another 24 hours. After that, more MTT-containing media was added, bringing the total MTT concentration to 0.5 mg/ml. At 37°C, the cells were cultured for a further 4 hours. Following a 4-hour incubation period, the medium was extracted and 100 μl of DMSO was used to dissolve the MTT formazan that was generated by living cells. A microplate reader was used to measure each well's absorbance at 570 nm.

Relative cell viability (%) was computed using the absorbance values from the wells treated with the sample and the control. The data's average standard deviation (SD), derived from three measurements done in duplicate, is given. The purpose of the experimental design and analysis was to evaluate the sample's effect on cell viability in a regulated in vitro setting.

2.4.4 Contact angle

This study aimed to find the longest scaffold duration which is necessary to enhance hydrophilicity and cell adhesion. The contact angle of droplets was applied on the surface 2 cm \times 2 cm utilizing the Young Laplace fitting method taking in to the account the ASTM D5946-04 requirements.

During this test, water droplets were put on the films' surface, then the contact angle was electronically recorded five seconds later. Three measurements were made for each sample to guarantee accuracy and dependability. Then the average was made.

2.4.5 Antibacterial activity

The antibacterial activity of the films was assessed using *Staphylococcus aureus* (*S. aureus*) bacteria and agar plate diffusion technique. The plates were incubated in the presence of a 5% CO_2 flow for a whole day. Then, the inhibitory zone was identified. The area surrounding the films where *Staphylococcus aureus* growth is impeded is known as the inhibition zone, and it serves as a measure of how well the films restrict bacterial activity. This approach offers gratitude information about the antibacterial capabilities of the film against these bacteria.

3. RESULTS AND DISCUSSION

3.1 Field emission scanning electron microscopy observations

Figure 3 illustrates the morphology of scaffold-coated nanofibers. The substrate's FESEM image (Figure 3a) (FA, 4%Alg) displays a uniform surface of alginate, which is ideal substrate for supporting electrospun nanofibers.

The dense nanofibers of samples FA1(4%Alg + 7%PVA), FA2(4%Alg + 7%PVA + 0.1%wt AgNPS), FA3(4%Alg + 7%PVA + 0.2%wt AgNPS), and FA4(4%Alg + 7%PVA + 0.3%wt AgNPS) at magnifications of 5 kX and 70 kX, respectively, are shown in the SEM images of Figures 3 b-c, d-e, f-g, h-i. These images show evidence of notable fiber crosslinking within the scaffolds.

The electrospinning solutions and conditions employed resulted in a reasonably broad distribution of fiber diameters. The fiber diameter sizes, ranging around 20-200 nm, are presented in magnification 70 kX. Notably, scaffolds with minimal or no beads exhibited improvements in nanofiber distribution, diameter, density, and electrospinning quality, showcasing enhanced density, nanofiber homogeneity, and smoother fibers. Fiber dimensions varied based on the solution

composition, with key factors influencing higher nanofiber densities including flow rate (1 h/ml), voltage (25 kV), and the distance between the collector and needle. Figure 4 illustrates the size distribution of uniformly generated nanofibers, ranging from 20 to 200 nm. Figure 4a for sample FA1(4%Alg + 7%PVA) showcases high average PVA nanofibers measuring about 280 nm. In the case of PVA-AgNPs (FA1(4%Alg + 7%PVA), FA2(4%Alg + 7%PVA + 0.1%wt AgNPS), FA3(4%Alg + 7%PVA + 0.2%wt AgNPS), and FA4(4%Alg + 7%PVA + 0.3%wt AgNPS), the inclusion of antibacterial agent dispersions led to less uniform fibers with reduced nanofiber diameters in the ranges of 112, 71, and 67 nm (Figures 3b-d). This reduction can be attributed to the addition of aqueous dispersions, which decreases the viscosity of electrospinning solutions.

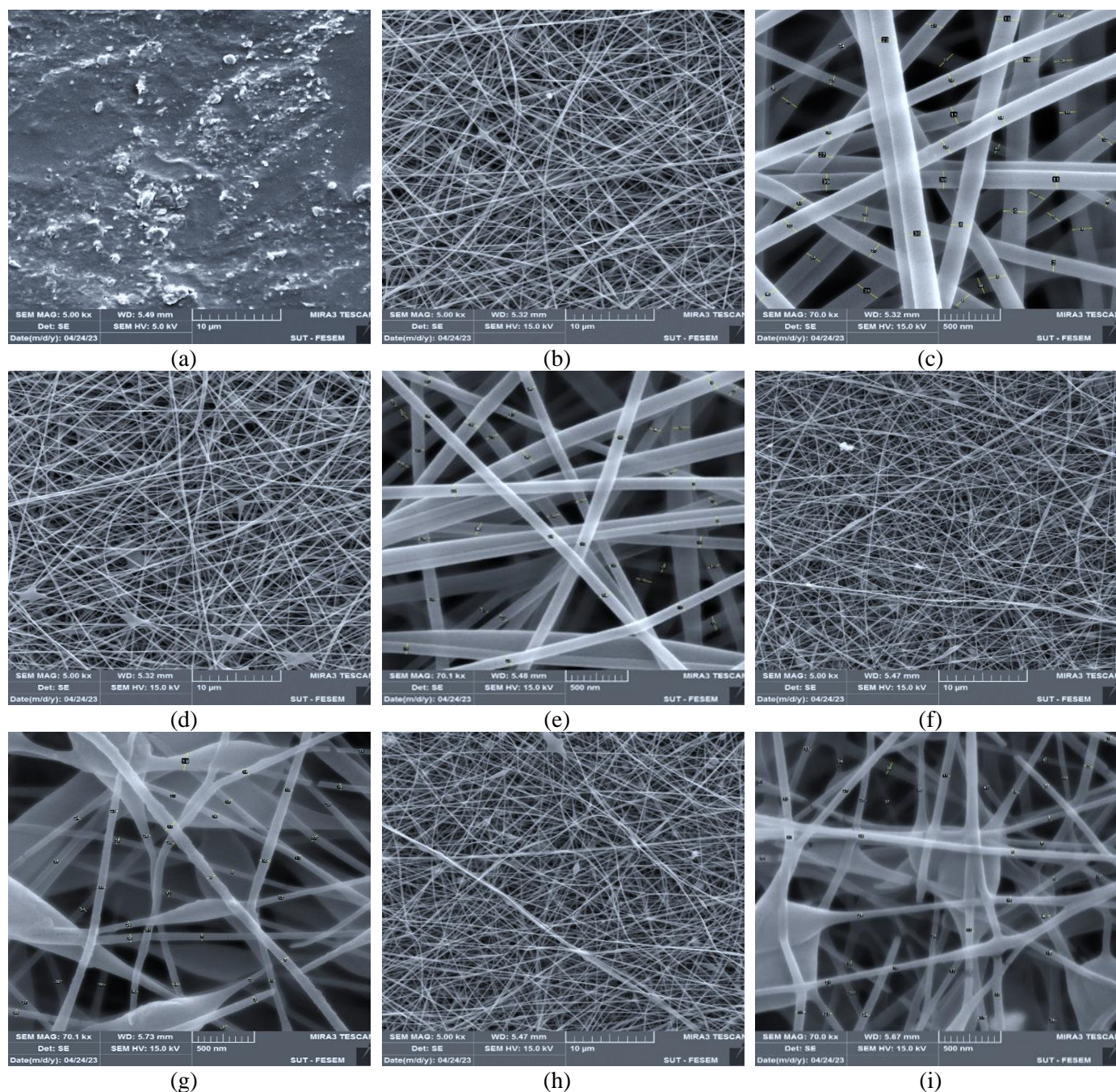


Figure 3. FESEM images of samples at magnification 5 and 70 kX respectively

Note: (a) FA; (b, c) FA1; (d, e) FA2; f, g) FA3; (h, i) FA4

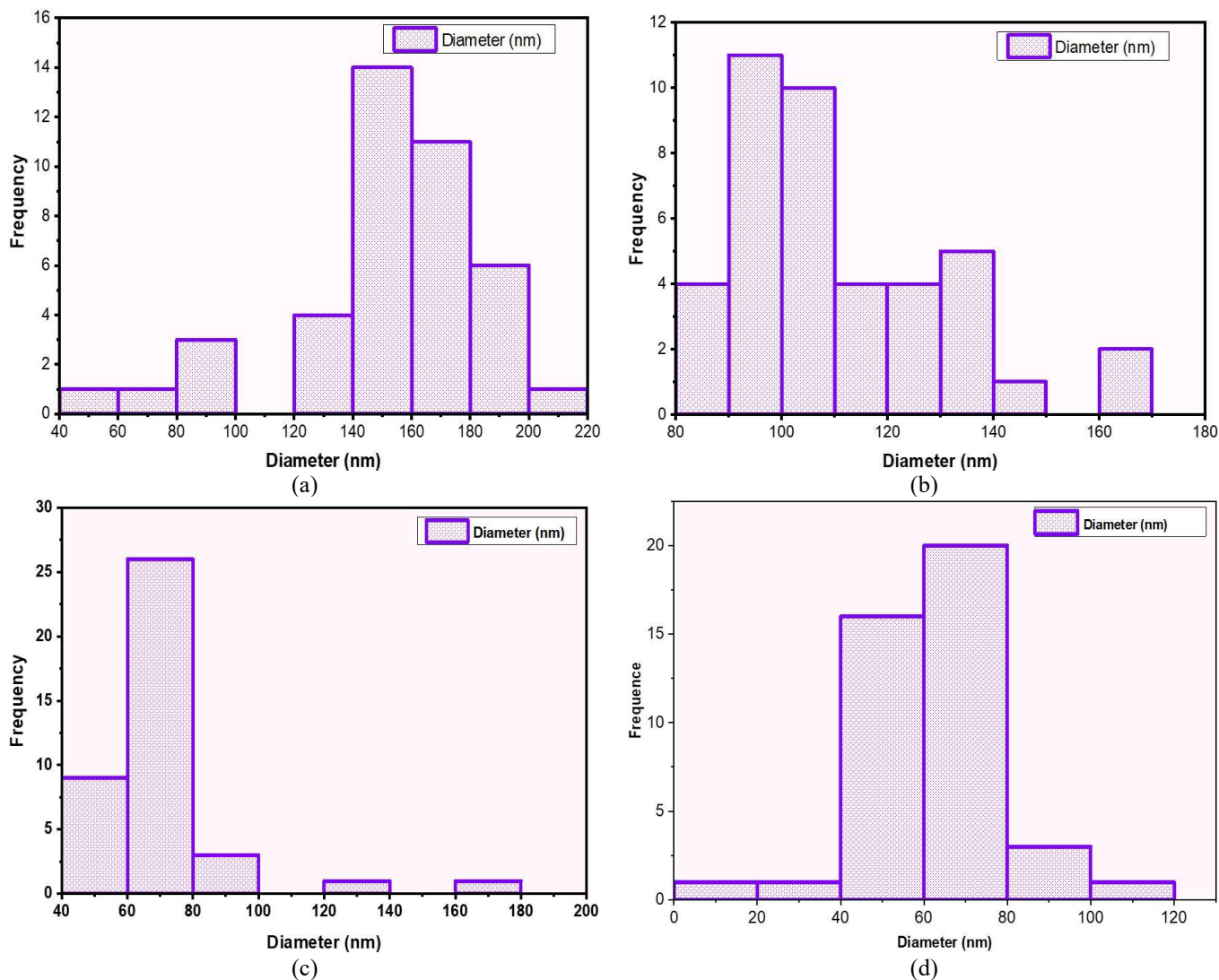


Figure 4. Average diameter of scaffolds

Note: (a) FA1 (4%Alg + 7%PVA); (b) FA2 (4%Alg + 7%PVA + 0.1%wt AgNPS); (c) FA3 (4%Alg + 7%PVA + 0.2%wt AgNPS); (d) FA4 (4%Alg + 7%PVA + 0.3%wt AgNPS)

3.2 Fourier transform infrared analysis

The FTIR spectrum of the sodium alginate substrate exhibits characteristic peaks at 1078 cm^{-1} , corresponding to the C-O-C stretching attributable to the alginate saccharide structure. Additional peaks are observed at 3277 cm^{-1} (OH-stretching) and 1600 cm^{-1} and 1414 cm^{-1} representing the stretching of carboxylate salt groups in an asymmetric and symmetric manner, respectively. These distinctive peaks are also evident in all coated nanostructures (Figure 5) [26].

In the spectra of SA-PVA, SA-PVA-0.1AgNPs, SA-PVA-0.2AgNPs, and SA-PVA-0.3AgNPs, peaks around 1602 cm^{-1} , 1600 cm^{-1} , 1551 cm^{-1} , and 1540 cm^{-1} , respectively, affirm the presence of sodium alginate in all coated nanostructures. The addition of AgNPs to SA/PVA induces changes in the vibration modes in a manner consistent with the expected alterations. The FTIR spectra indicate significant alterations in the intensity and shape of the observed bands, while the shifts in the bands have a limited impact on spectrum interpretation. Notably, the band corresponding to symmetric vibrations exhibits a shift to a higher value, specifically at 1418 cm^{-1} . These results suggest that the addition of AgNPs to the scaffold has varying impacts on spatial organization and overall interactions within the nanofiber, with contributions that are balanced to some extent [27].

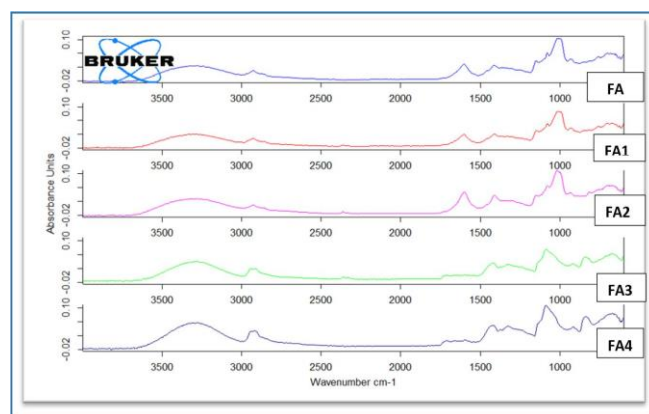


Figure 5. FTIR of scaffolds

Note: FA: 4%Alg, FA1: 4%Alg + 7%PVA, FA2: 4%Alg + 7%PVA + 0.1%wt AgNPS, FA3: 4%Alg + 7%PVA + 0.2%wt AgNPS, FA4: 4%Alg + 7%PVA + 0.3%wt AgNPS)

3.3 Contact angle

The wettability of scaffolds is crucial for promoting cell attachment and adhesion, particularly in the context of tissue engineering applications where hydrophilicity is desirable.

Figure 6 illustrates the static water contact angles of the SA/PVA/AgNPs scaffolds, and Figure 7 presents images of contact angle measurements for each sample.

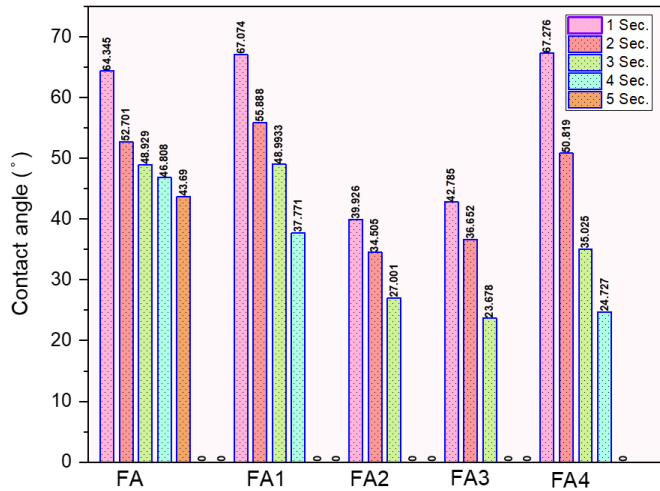


Figure 6. Contact angle of scaffolds

Note: FA: 4%Alg, FA1: 4%Alg + 7%PVA, FA2: 4%Alg + 7%PVA + 0.1%wt AgNPS, FA3: 4%Alg + 7%PVA + 0.2%wt AgNPS, FA4: 4%Alg + 7%PVA + 0.3%wt AgNPS

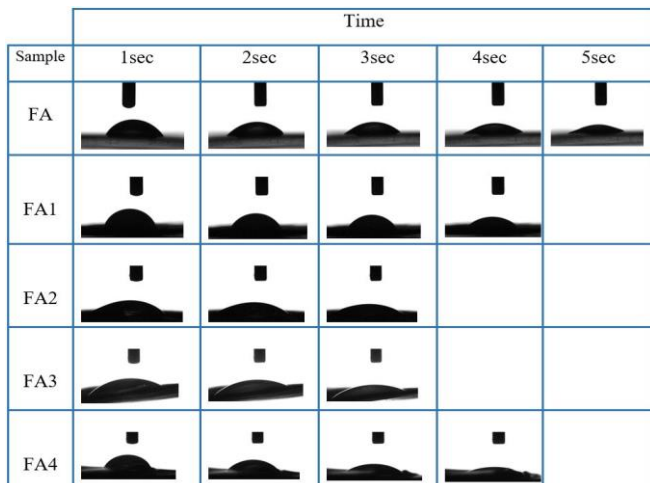


Figure 7. Images of contact angle of scaffolds

Note: FA: 4%Alg, FA1: 4%Alg + 7%PVA, FA2: 4%Alg + 7%PVA + 0.1%wt AgNPS, FA3: 4%Alg + 7%PVA + 0.2%wt AgNPS, FA4: 4%Alg + 7%PVA + 0.3%wt AgNPS

The contact angle of the sodium alginate substrate (FA) is measured at 64.3345, indicating hydrophilic behavior. As the composition of sodium alginate is modified, the contact angle decreases. For example, the contact angle (FA1) of an alginate substrate coated with polyvinyl alcohol nanofibers is 67.074, suggesting sustained hydrophilicity over time. With the introduction of polyvinyl alcohol nanofibers reinforced with AgNPs in FA2, FA3, and FA4, the contact angles decrease to 39.926°, 42.785°, and 67.276°, respectively. This decrease in contact angle after alginate coating indicates that the scaffold surfaces become more hydrophilic than before coating.

A contact angle below 90 degrees is indicative of hydrophilicity, and all scaffolds exhibit low contact angles, making them well-suited for cell attachment. The hydrophilic nature of these scaffolds, attributed to the combination of sodium alginate substrate and polyvinyl alcohol nanofibers reinforced with AgNPs, enhances their suitability for promoting cell interactions in tissue engineering applications.

3.4 Antibacterial activity

Figure 8 illustrates the antimicrobial efficacy of coated nanofibers against *S. aureus* bacteria, and the corresponding zone of inhibition is presented in Figure 9. The results underscore the broad-spectrum antibacterial activity of these scaffolds against Gram-positive *S. aureus* bacteria. Notably, plates with SA substrate films exhibited minimal antimicrobial activity during the specified period.

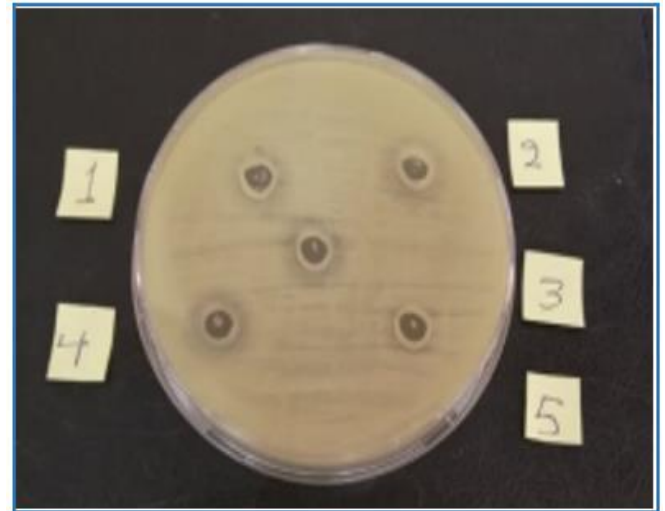


Figure 8. Antibacterial activity for scaffolds

Note: 1) FA, 2) FA1, 3) FA2, 4) FA3, 5) FA4

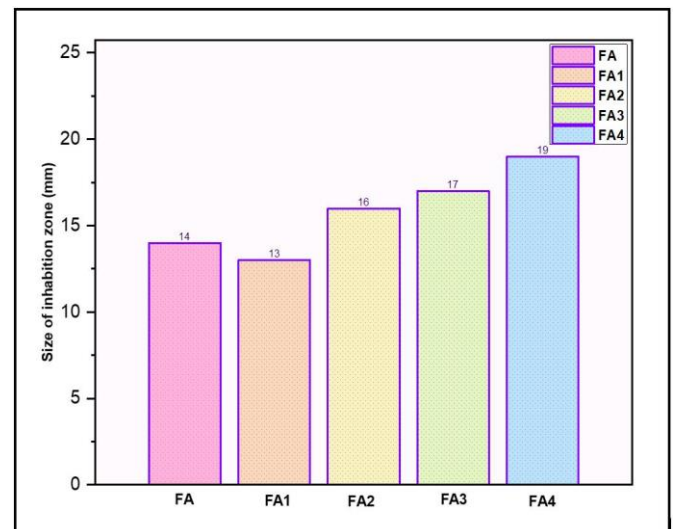


Figure 9. Size of inhibition zone of scaffolds

Note: FA: 4%Alg, FA1: 4%Alg + 7%PVA, FA2: 4%Alg + 7%PVA + 0.1%wt AgNPS, FA3: 4%Alg + 7%PVA + 0.2%wt AgNPS, FA4: 4%Alg + 7%PVA + 0.3%wt AgNPS

The antimicrobial activity of (SA/PVA/AgNPs) with various concentrations of AgNPs against *S. aureus* demonstrated a more substantial inhibition zone compared to SA alone. This increased inhibitory effect is attributed to the presence of silver nanoparticles (AgNPs) in the scaffold.

In particular, silver nanoparticles are one of the noble metals whose antibacterial properties have been well studied. Among the diseases against which the nanoparticles exhibit high resistance are bacteria resistant to antibiotics. When polymers are coupled with other antibacterial agents such as silver ions

and antimicrobial peptides, their good antibacterial properties become evident [28].

The well-documented broad-spectrum antibacterial properties of silver are based on the premise that human cells are significantly less susceptible to its toxicity than microorganisms. The cumulative impact of the intricate interactions between the silver ions and cellular structures or components determines the specific effects on the growth of a given microorganism [29].

3.5 Cell viability

Figure 10 presents the cell viability results at 24h, 48h, and 72h. The cell adhesion assay indicates high cell attachment on the scaffolds. The MTT findings for all tested materials at 24h, 48h, and 72h reveal excellent cytocompatibility. Scaffolds play a crucial role in tissue engineering, providing a conducive environment for cell attachment and growth. The created scaffold (SA/PVA/AgNPs) appears to enhance cell viability, with cell viability percentages reaching up to 85% after 72h of cell culture.

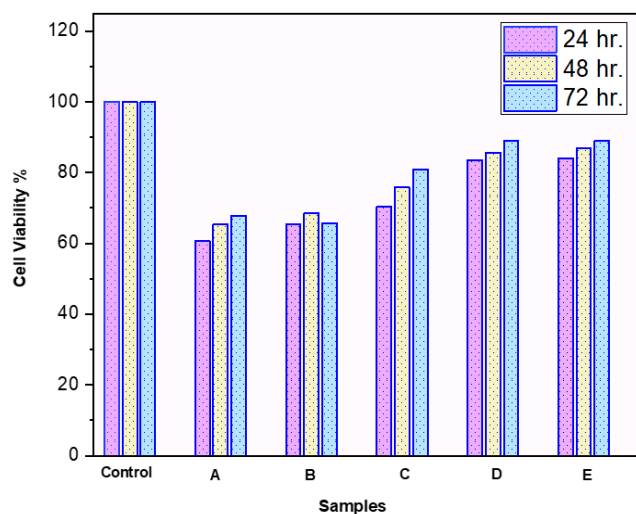


Figure 10. Cell viability of scaffolds at 24h, 48h, and 27h

Note: A: 4%Alg, B: 4%Alg + 7%PVA, C: 4%Alg + 7%PVA + 0.1%wt AgNPS, D: 4%Alg + 7%PVA + 0.2%wt AgNPS, E: (4%Alg + 7%PVA + 0.3%wt AgNPS

The cell viability of (SA/PVA/AgNPs 0.1, 0.2, 0.3 g) shows a slight increase after 72h, and the percentages are maintained above 80%, indicating a non-toxic effect. Previous research on the biocompatibility of polyvinyl alcohol (PVA) suggested that pure PVA could have slight harmful effects on surrounding tissues. However, it is noted that the biocompatibility of PVA can be improved by combining it with other biocompatible polymers, such as natural polymers like collagen, chitosan, alginate, and gelatin [30-32]. This underscores the importance of the scaffold composition in influencing cell behavior and overall biocompatibility in tissue engineering applications.

The films coated with nanofibers can be used in the discipline of tissue engineering for applications in skin tissue engineering.

4. CONCLUSION

The objective of preparing and analyzing these scaffolds as potential candidates for skin tissue engineering was to assess

the unique coated nanofibers, which are based on electrospun polyvinyl alcohol with antimicrobial agents, and placed onto alginate films. All coated nanofibers retained the distinctive sodium alginate structure peaks, as confirmed by the FT-IR study, indicating the preservation of the polyvinyl alcohol structure on the substrate. In accordance with the results, at a flow rate of 1 h/ml, voltage of 25 kV, and a distance of 15 cm between the collector and needle, uniform and homogeneous nanofibers with a regular size distribution and a narrow diameter (20 to 200 nm) developed. Because of the combination of AgNP-reinforced polyvinyl alcohol nanofibers and sodium alginate substrate, these scaffolds are hydrophilic, which makes them more suitable for encouraging cell interactions in tissue engineering applications.

Both the sodium alginate substrate and the coated nanofibers (PVA-AgNPs) exhibited good biocompatibility, as evidenced by in vitro cytotoxicity assessments.

The manufactured scaffolds demonstrated favorable physiochemical and biological characteristics under these conditions, suggesting their suitability for skin tissue engineering applications. The incorporation of antimicrobial agents in the form of AgNPs enhances the potential of these scaffolds for skin tissue engineering by providing antibacterial properties, which is crucial for promoting a healthy tissue environment.

REFERENCES

- [1] Pandey, A.R., Singh, U.S., Momin, M., Bhavsar, C. (2017). Chitosan: Application in tissue engineering and skin grafting. *Journal of Polymer Research*, 24: 1-22. <https://doi.org/10.1007/s10965-017-1286-4>
- [2] Kadhim, I.A.U., Sallal, H.A., Al-Khafaji, Z.S. (2023). A review in investigation of marine biopolymer (chitosan) for bioapplications. *ES Materials & Manufacturing*, 21: 828. <https://doi.org/10.30919/esmm5f828>
- [3] Pina, S., Ribeiro, V.P., Marques, C.F., Maia, F.R., Silva, T.H., Reis, R.L., Oliveira, J.M. (2019). Scaffolding strategies for tissue engineering and regenerative medicine applications. *Materials*, 12(11): 1824. <https://doi.org/10.3390/ma12111824>
- [4] Kadhim, I.A.U. (2023). Investigation of physiochemical and biological properties of composite sodium alginate for tissue engineering. *Journal of Biomimetics, Biomaterials and Biomedical Engineering*, 59: 11-20. <https://doi.org/10.4028/p-a7ygw7>
- [5] Kadhim, I.A., Ameer, Z.J.A., Alzubaidi, A.B. (2020). Investigation of chitosan film degradation in tissue engineering applications. In *IOP Conference Series: Materials Science and Engineering*, 671(1): 012060. <https://doi.org/10.1088/1757-899X/671/1/012060>
- [6] Kadhim, I.A.U. (2021). Biocompatibility of alginate-graphene oxide film for tissue engineering applications. *Key Engineering Materials*, 900: 26-33. <https://doi.org/10.4028/www.scientific.net/KEM.900.26>
- [7] Bhattarai, D.P., Aguilar, L. E., Park, C. H., & Kim, C. S. (2018). A review on properties of natural and synthetic based electrospun fibrous materials for bone tissue engineering. *Membranes*, 8(3): 62. <https://doi.org/10.3390/membranes8030062>
- [8] Kadhim, A.A., Alameer, Z.J.A., Zubaidi, A.B.A. (2019). Enzymatic degradation of chitosan blend for tissue engineering application. In *AIP Conference Proceedings*,

- Beirut, Lebanon. <https://doi.org/10.1063/1.5116944>
- [9] Abasalizadeh, F., Moghaddam, S.V., Alizadeh, E., Akbari, E., Kashani, E., Fazljou, S.M.B., Akbarzadeh, A. (2020). Alginate-based hydrogels as drug delivery vehicles in cancer treatment and their applications in wound dressing and 3D bioprinting. *Journal of biological engineering*, 14: 1-22. <https://doi.org/10.1186/s13036-020-0227-7>
- [10] Jönsson, M., Allahgholi, L., Sardari, R.R., Hreggviðsson, G.O., Nordberg Karlsson, E. (2020). Extraction and modification of macroalgal polysaccharides for current and next-generation applications. *Molecules*, 25(4): 930. <https://doi.org/10.3390/molecules25040930>
- [11] Montalbano, G., Toumpaniari, S., Popov, A., Duan, P., Chen, J., Dalgarno, K., Ferreira, A.M. (2018). Synthesis of bioinspired collagen/alginate/fibrin based hydrogels for soft tissue engineering. *Materials Science and Engineering: C*, 91: 236-246. <https://doi.org/10.1016/j.msec.2018.04.101>
- [12] Beltran-Vargas, N.E., Peña-Mercado, E., Sánchez-Gómez, C., Garcia-Lorenzana, M., Ruiz, J.C., Arroyo-Maya, I., Campos-Terán, J. (2022). Sodium alginate/chitosan scaffolds for cardiac tissue engineering: The influence of its three-dimensional material preparation and the use of gold nanoparticles. *Polymers*, 14(16): 3233. <https://doi.org/10.3390/polym14163233>
- [13] Barbon, S., Contran, M., Stocco, E., Todros, S., Macchi, V., Caro, R.D., Porzionato, A. (2021). Enhanced biomechanical properties of polyvinyl alcohol-based hybrid scaffolds for cartilage tissue engineering. *Processes*, 9(5): 730. <https://doi.org/10.3390/pr9050730>
- [14] Rasyida, A., Halimah, S., Wijayanti, I.D., Wicaksono, S.T., Nurdiansah, H., Silaen, Y.M.T., Purniawan, A. (2023). A composite of hydrogel alginate/PVA/r-GO for scaffold applications with enhanced degradation and biocompatibility properties. *Polymers*, 15(3): 534. <https://doi.org/10.3390/polym15030534>
- [15] Thurzo, A., Gálfiová, P., Nováková, Z.V., Polák, Š., Varga, I., Strunga, M., Danišovič, L. (2022). Fabrication and in vitro characterization of novel hydroxyapatite scaffolds 3D printed using polyvinyl alcohol as a thermoplastic binder. *International Journal of Molecular Sciences*, 23(23): 14870. <https://doi.org/10.3390/ijms232314870>
- [16] Mihai, M.M., Dima, M.B., Dima, B., Holban, A.M. (2019). Nanomaterials for wound healing and infection control. *Materials*, 12(13): 2176. <https://doi.org/10.3390/ma12132176>
- [17] Jeckson, T.A., Neo, Y.P., Sisinthy, S.P., Gorain, B. (2021). Delivery of therapeutics from layer-by-layer electrospun nanofiber matrix for wound healing: An update. *Journal of Pharmaceutical Sciences*, 110(2): 635-653. <https://doi.org/10.1016/j.xphs.2020.10.003>
- [18] Zhong, S., Zhang, Y., Lim, C.T. (2012). Fabrication of large pores in electrospun nanofibrous scaffolds for cellular infiltration: A review. *Tissue Engineering Part B: Reviews*, 18(2): 77-87. <https://doi.org/10.1089/ten.teb.2011.0390>
- [19] Makvandi, P., Wang, C.Y., Zare, E.N., Borzacchiello, A., Niu, L.N., Tay, F.R. (2020). Metal-based nanomaterials in biomedical applications: Antimicrobial activity and cytotoxicity aspects. *Advanced Functional Materials*, 30(22): 1910021. <https://doi.org/10.1002/adfm.201910021>
- [20] Tyner, K.M., Zou, P., Yang, X., Zhang, H., Cruz, C.N., Lee, S.L. (2015). Product quality for nanomaterials: Current US experience and perspective. *Wiley Interdisciplinary Reviews: Nanomedicine and Nanobiotechnology*, 7(5): 640-654. <https://doi.org/10.1002/wnan.1338>
- [21] Gao, Y., Shao, W., Qian, W., He, J., Zhou, Y., Qi, K., Wang, R. (2018). Biomaterialized poly (l-lactic-co-glycolic acid)-tussah silk fibroin nanofiber fabric with hierarchical architecture as a scaffold for bone tissue engineering. *Materials Science and Engineering: C*, 84: 195-207. <https://doi.org/10.1016/j.msec.2017.11.047>
- [22] Vazquez-Muñoz, R., Meza-Villezas, A., Fournier, P.G.J., Soria-Castro, E., Juárez-Moreno, K., Gallego-Hernández, A.L., Huerta-Saquero, A. (2019). Enhancement of antibiotics antimicrobial activity due to the silver nanoparticles impact on the cell membrane. *PloS One*, 14(11): e0224904. <https://doi.org/10.1371/journal.pone.0224904>
- [23] Jian, Y., Chen, X., Ahmed, T., Shang, Q., Zhang, S., Ma, Z., Yin, Y. (2022). Toxicity and action mechanisms of silver nanoparticles against the mycotoxin-producing fungus *Fusarium graminearum*. *Journal of Advanced Research*, 38: 1-12. <https://doi.org/10.1016/j.jare.2021.09.006>
- [24] Khan, M.U.A., Al-Thebaiti, M.A., Hashmi, M.U., Aftab, S., Abd Razak, S.I., Abu Hassan, S., Amin, R. (2020). Synthesis of silver-coated bioactive nanocomposite scaffolds based on grafted beta-glucan/hydroxyapatite via freeze-drying method: Anti-microbial and biocompatibility evaluation for bone tissue engineering. *Materials*, 13(4): 971. <https://doi.org/10.3390/ma13040971>
- [25] Burduşel, A.C., Gherasim, O., Grumezescu, A.M., Mogoantă, L., Ficai, A., Andronescu, E. (2018). Biomedical applications of silver nanoparticles: an up-to-date overview. *Nanomaterials*, 8(9): 681. <https://doi.org/10.3390/nano8090681>
- [26] Iqbal, B., Muhammad, N., Jamal, A., Ahmad, P., Khan, Z.U.H., Rahim, A., Rehman, I.U. (2017). An application of ionic liquid for preparation of homogeneous collagen and alginate hydrogels for skin dressing. *Journal of Molecular Liquids*, 243: 720-725. <https://doi.org/10.1016/j.molliq.2017.08.101>
- [27] Vidovic, S., Stojkowska, J., Stevanovic, M., Balanc, B., Vukasinovic-Sekulic, M., Marinkovic, A., Obradovic, B. (2022). Effects of poly (vinyl alcohol) blending with Ag/alginate solutions to form nanocomposite fibres for potential use as antibacterial wound dressings. *Royal Society Open Science*, 9(3): 211517. <https://doi.org/10.1098/rsos.211517>
- [28] Susilowati, E., Mahardiani, L., Hardini, R.D. (2022). The effect of silver nanoparticles toward properties and antibacterial activity of silver-alginate nanocomposite films. *Frontiers in Sustainable Food Systems*, 6: 913750. <https://doi.org/10.3389/fsufs.2022.913750>
- [29] Cheon, J.Y., Kim, S.J., Rhee, Y.H., Kwon, O.H., Park, W.H. (2019). Shape-dependent antimicrobial activities of silver nanoparticles. *International Journal of Nanomedicine*, 14: 2773-2780. <https://doi.org/10.2147/IJN.S196472>
- [30] Alexandre, N., Ribeiro, J., Gaertner, A., Pereira, T., Amorim, I., Fragoso, J., Luis, A.L. (2014). Biocompatibility and hemocompatibility of polyvinyl

- alcohol hydrogel used for vascular grafting—In vitro and in vivo studies. *Journal of biomedical materials research Part A*, 102(12): 4262-4275. <https://doi.org/10.1002/jbm.a.35098>
- [31] Khalaji, S., Golshan Ebrahimi, N., Hosseinkhani, H. (2021). Enhancement of biocompatibility of PVA/HTCC blend polymer with collagen for skin care application. *International Journal of Polymeric Materials and Polymeric Biomaterials*, 70(7): 459-468. <https://doi.org/10.1080/00914037.2020.1725761>
- [32] Jadbabaei, S., Kolahdoozan, M., Naeimi, F., Ebadi-Dehaghani, H. (2021). Preparation and characterization of sodium alginate–PVA polymeric scaffolds by electrospinning method for skin tissue engineering applications. *RSC Advances*, 11(49): 30674-30688. <https://doi.org/10.1039/D1RA04176B>